Hadron physics with polarized photons at LEPS/LEPS2

Sun Young Ryu

(RCNP, Osaka University)

EMMI

New Vistas in Photon Physics in Heavy-Ion Collisions

Sep 19 – 22, 2022
Institute of Nuclear Physics Polish Academy of Sciences & AGH University of Science and Technology

Outline

1. Compton-backscattered photon beam
2. Highlights from the LEPS experiments: photoproduction of $(\pi,\ \eta,\ \eta',\ K^+)$ mesons and $(\omega,\ \phi,\ K^*)$ mesons.
3. Current status of the LEPS2 photoproduction experiments: photoproduction of η and ω mesons with BGOegg detector.
4. Search for Θ^+, P_s and K^-pp with the LEPS2 detector.

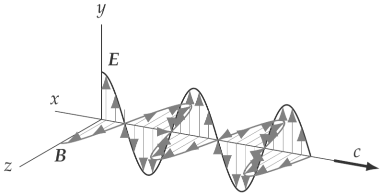

GeV γ

Photon Beam

- Because of a small attenuation of the photon inside the nucleon the photon is an ideal probe to explore the interior of the hadrons.
- The largest γp total cross section is $\sigma \approx 520\mu$b at $E_\gamma \approx 0.32$ GeV, which corresponds to a mean free path for a photon in nuclear matter much larger than the nuclear radius ($\lambda \approx 100$ fm).
- At low masses, the $\Delta(1232)$ resonance, the first excited state, can be clearly observed as a peak in the cross section for $p\pi^0$. All other structures are not composites of a single resonant state, but arise due to several overlapping states. [a]

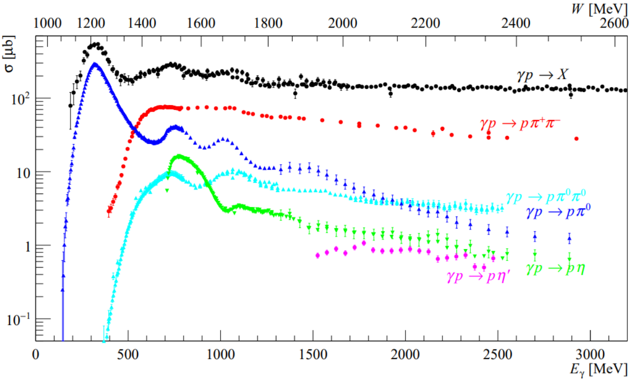

[a] A. Thiel, F. Afzal, and Y. Wunderlich, Prog. Part. Nucl. Phys. 125, 103949 (2022).

Backward Compton Scattering

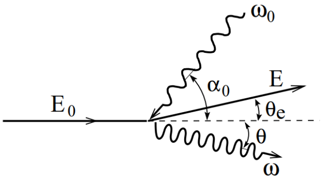

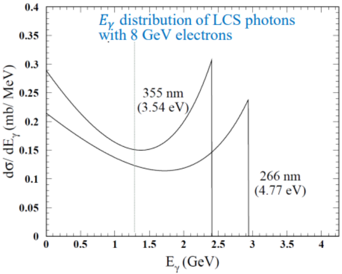

- Kinematics of the backward Compton scattering $e(p_0) + \gamma_0(k_0) \rightarrow e(p) + \gamma(k)$ is characterized by two dimensionless variables x and y: [a]

$$x = \frac{2p_0 k_0}{m^2c^2} \approx \frac{4E_0\omega_0}{m^2c^4}\cos^2\frac{\alpha_0}{2}. \qquad y = \frac{kk_0}{p_0}k_0 \approx \frac{\omega}{E_0}$$

- The maximum energy of the scattered photon ω_m and the maximum value of the parameter y are:

$$\omega \le \omega_m = \frac{x}{x+1}E_0, \qquad y \le y_m = \frac{x}{x+1} = \frac{\omega_m}{E_0}$$

- The energy spectrum of Compton backscattered photons is given by:

$$\frac{d\sigma}{dy} \approx \frac{2\sigma_0}{x}\left[\frac{1}{1-y} + 1 - y - 4r(1-r)\right], \qquad \text{where } r = \frac{y}{x(1-y)} \le 1.$$

[a] V.G. Serbo, Acta Phys. Polon. B 37, 1333 (2006)

Backward Compton Scattering

- The energy range of Compton backscattered photons spans $E_\gamma = 1.4$–2.9 GeV at SPring-8, which fits the extensive study of baryon resonances near 2 GeV. Note that photons from UPC are produced at much higher energies ($E_\gamma = \gamma\hbar c/R_A \approx 3$ GeV @ Au+Au at $\sqrt{s_{NN}} = 200$ GeV and $E_\gamma = \gamma\hbar c/R_A \approx 75$ GeV @ Pb+Pb at $\sqrt{s_{NN}} = 5.02$ TeV). [a]
- The energy of a Compton backscattered photon depends on its emission angle θ:

$$\omega = \frac{\omega_m}{1+(\theta/\theta_0)^2}, \qquad \theta_0 = \frac{mc^2}{E_0}\sqrt{x+1}$$

- If the laser light is polarized, then high-energy photons are polarized in the same direction, which is characterized by:

$$x = \frac{4E_0\omega_0}{m^2c^4}, \qquad a = \frac{1}{1+x}, \qquad \rho = \frac{\omega}{\omega_m}, \qquad k = \frac{\rho^2(1-a)^2}{1-\rho(1-a)}, \qquad \cos\theta_0 = \frac{1-\rho(1+a)}{1-\rho(1-a)}$$

  At the Compton edge ($\omega = \omega_m$), $\rho = 1$, $\cos\theta_0 = -1$, and $k = (1-a^2)/a$.
- For linear polarization,

$$\frac{P_\gamma}{P_{\text{laser}}} = \frac{(1-\cos\theta_0)^2}{2(k+1+\cos^2\theta_0)} \underbrace{\longrightarrow}_{Compton-edge} \frac{2}{2+k} < 1$$

- For circular polarization,

$$\frac{P_\gamma}{P_{\text{laser}}} = \frac{(k+2)\cos\theta_0}{(k+1+\cos^2\theta_0)} \underbrace{\longrightarrow}_{Compton-edge} -1$$

[a] Mariusz Przybycien, "Overview of UPC Snowmass LoI physics cases", RHIC Science Programs, 2021

LEPS and LEPS2 at SPring-8

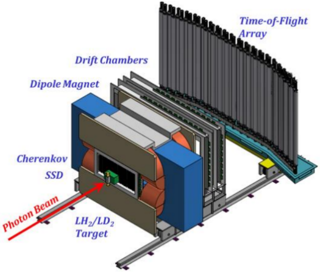

LEPS spectrometer

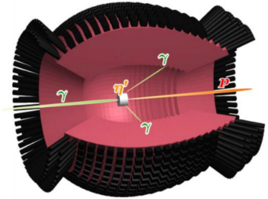

BGOegg calorimeter

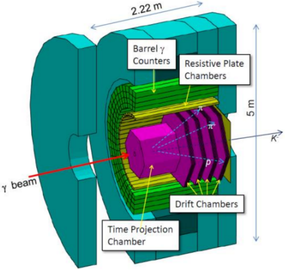

Solenoid spectrometer

	LEPS (2000 – 2020)	LEPS2 (2013 -)	
Tagged γ Energy	$1.5 < E_\gamma < 2.4$ GeV (UV laser) $1.5 < E_\gamma < 2.9$ GeV (DUV laser)	$1.3 < E_\gamma < 2.4$ GeV (UV laser) $1.3 < E_\gamma < 2.9$ GeV (DUV laser)	
Photon Beam Intensity	Two laser injection 2×10^6 cps (UV laser) 2×10^5 cps (UV laser)	Four laser injection $< 10^7$ cps (UV laser) $< 10^6$ cps (DUV laser)	
Detector	Forward Dipole Spectrometer	BGOegg EM Calorimeter	Solenoid Spectrometer

Photoproduction of Pseudoscalar Mesons

- Photoproduction of pseudoscalar mesons (π, η, η', K) is the simplest process to analyze.

$$\gamma + N \to \begin{bmatrix} \pi \\ \eta \\ \eta' \end{bmatrix} + N$$

$$\lambda = \pm 1 \quad m_s = \pm\frac{1}{2} \to \quad 0 \quad m_s = \pm\frac{1}{2}$$

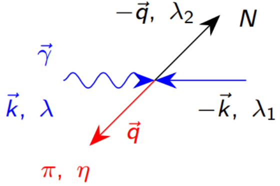

- Four spin degrees of freedom with four complex amplitudes, usually given as CGLN, helicity, or transversity amplitudes:

$$\mathfrak{F} = \chi^{\dagger}_{m_{s_f}} F_{\text{CGLN}} \chi_{m_{s_i}}$$

$$F_{\text{CGLN}} = i\vec{\sigma}\cdot\hat{\epsilon}F_1 + \vec{\sigma}\cdot\hat{q}\vec{\sigma}\cdot\hat{k}\times\hat{\epsilon}F_2 + i\vec{\sigma}\cdot\hat{k}\hat{q}\cdot\hat{\epsilon}F_3 + i\vec{\sigma}\cdot\hat{q}\hat{q}\cdot\hat{\epsilon}F_4$$

- From four complex amplitudes, one can construct 16 polarization observables, which can be measured with linearly or circularly polarized photon beams, polarized targets, and recoil polarization detection: single polarization observables ($\sigma_0 = d\sigma/d\Omega$, Σ, T, P), beam-target observables (E, F, G, H), beam-recoil observables ($C_{x'}$, $C_{z'}$, $O_{x'}$, $O_{z'}$), and target-recoil observables ($T_{x'}$, $T_{z'}$, $L_{x'}$, $L_{z'}$)

Light Baryon Spectroscopy

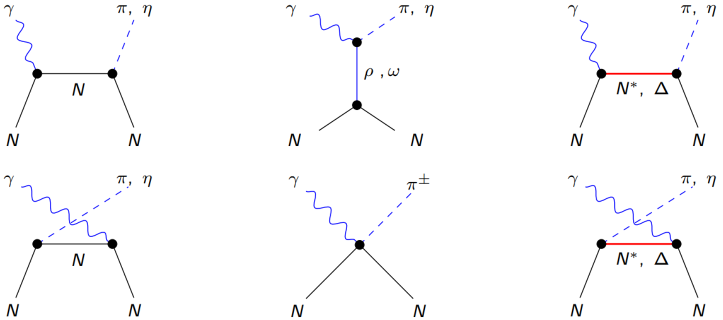

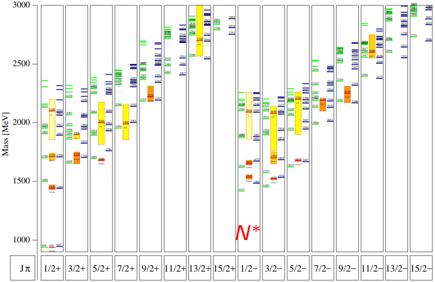

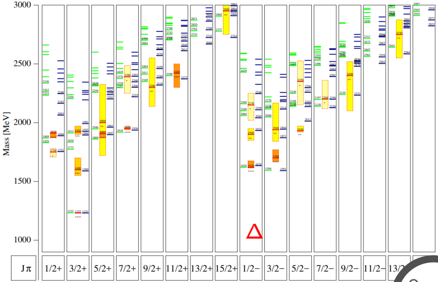

Backward π^0 Photoproduction

- Differential cross sections and photon beam asymmetries for π^0 photoproduction have been measured at $E_\gamma = 1.5$–2.4 GeV and at the π^0 scattering angles, $-1 < \cos\theta_{c.m.} < -0.6$.

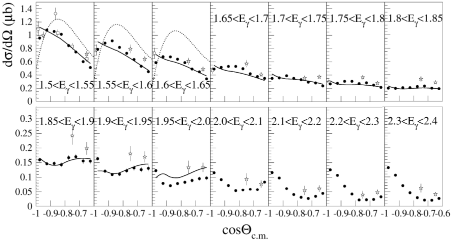

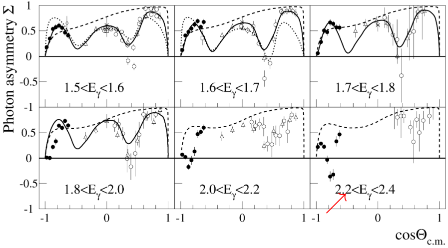

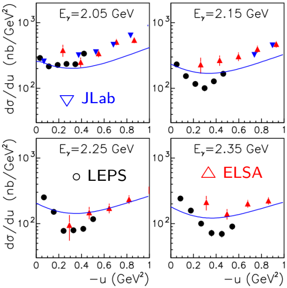

- Above 2.0 GeV, a dip structure around $\cos\theta_{c.m.} = -0.8$ requires new high-mass resonances combined with the u-channel diagrams. [a]

$$P_\gamma \Sigma \cos 2\Phi = \frac{nN_v - N_h}{nN_v + N_h}$$

- Regge contributions should come to play and interferences will occur. [b]

[a] M. Sumihama *et al.* (LEPS Collab), Phys. Lett. B 657, 32 (2007).
[b] A. Sibirtsev *et al.*, Eur. Phys. J A 40, 65 (2009).

Backward η Photoproduction

- Backward η photoproduction off protons has been measured at $E_\gamma = 1.6\text{–}2.4$ GeV at the SPring-8/LEPS facility, by detecting protons scattered at forward angles.

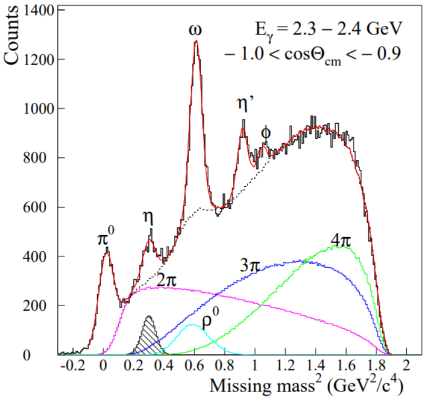

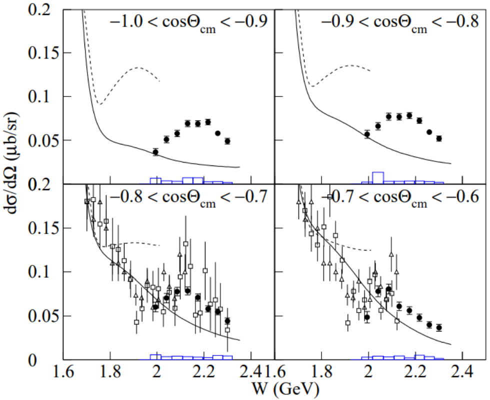

- This work provides unambiguous evidence for a bump structure above $W = 2.0$ GeV. No such structure is seen in η', ω and π^0 photoproductions, which supports that this unique structure in η photoproduction is due to a baryon resonance with a large $s\bar{s}$ component. [a]

[a] M. Sumihama *et al.* (LEPS Collab), Phys. Rev. C 80, 052201 (2009).

ϕ Photoproduction near Threshold

- In the vector meson dominance (VMD) model for photoproduction, a real photon can fluctuate into a virtual vector meson $V = \{\rho, \omega, \phi\}$, which subsequently scatters off the target proton.
- The ϕ meson production has the unique feature within gluon dynamics of being a result of OZI suppression due to the dominant $\bar{s}s$ structure.

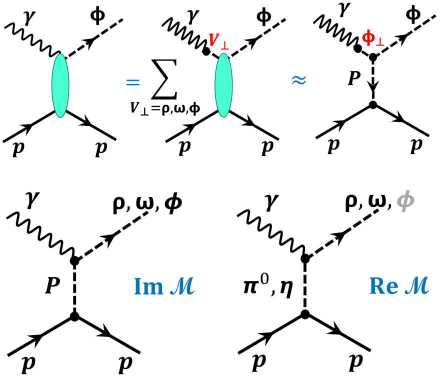

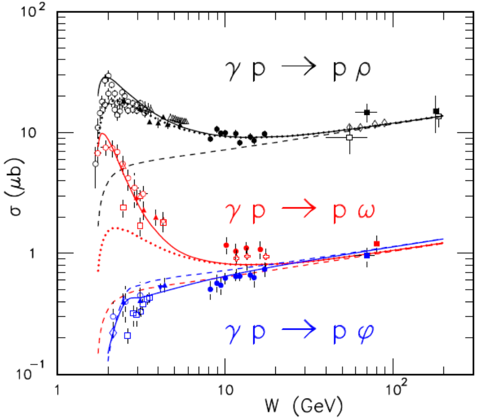

ϕ Photoproduction near Threshold

- For Pomeron exchanges, the photoproduction cross section can be written in the form

$$\frac{d\sigma}{dt}(\gamma p \to \phi p) = \left(\frac{d\sigma}{dt}\right)_{t=t_{\min}} \exp(-b_\phi |t - t_{\min}|)$$

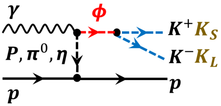

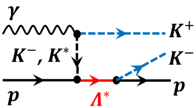

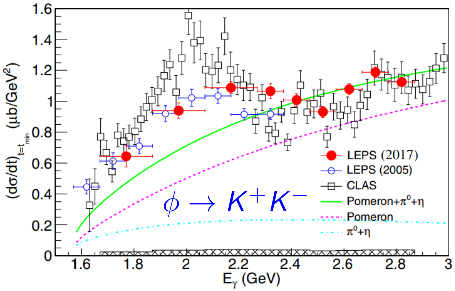

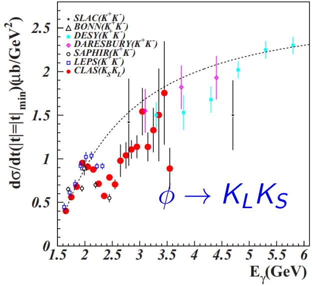

- Differential cross sections for ϕ photoproduction in the reaction $\gamma p \to p\phi$ followed by $\phi \to K^+K^-$ [a] and $K_S K_L$ [b] show some enhancement in the photon beam energy range near 2.1 GeV.

---

[a] K. Mizutani *et al.* (LEPS Collab), PRC 96, 062201(*R*)(2017); B. Dey *et al.* (CLAS Collab), PRC 89, 055208(2014)

[b] H. Seraydaryan *et al.* (CLAS Collab), PRC 89, 055206(2014).

Decay Angular Distribution and SDMEs

$\gamma p \to \phi p$

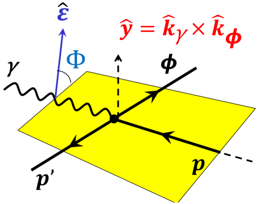

$$W(\cos\theta) = \frac{3}{2}\left(\frac{1}{2}(1-\rho^0_{00})\sin^2\theta + \rho^0_{00}\cos^2\theta\right)$$

$$W(\phi) = \frac{1}{2\pi}(1 - 2\rho^0_{1-1}\cos 2\phi)$$

$$W(\phi-\Phi) = \frac{1}{2\pi}\left(1 + P_\gamma(\rho^1_{1-1} - \mathrm{Im}\rho^2_{1-1})\cos 2(\phi-\Phi)\right)$$

$$W(\phi+\Phi) = \frac{1}{2\pi}\left(1 + P_\gamma(\rho^1_{1-1} + \mathrm{Im}\rho^2_{1-1})\cos 2(\phi+\Phi)\right)$$

$$W(\Phi) = 1 - P_\gamma(2\rho^1_{11} + \rho^1_{00})\cos 2\Phi$$

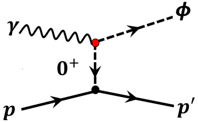

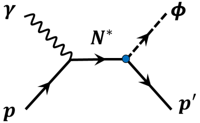

$$P_\sigma = \frac{\sigma^N - \sigma^U}{\sigma^N + \sigma^U} = 2\rho^1_{1-1} - \rho^1_{00}$$

$$\Sigma = \frac{\sigma_\parallel - \sigma_\perp}{\sigma_\parallel + \sigma_\perp} = \frac{\rho^1_{11} + \rho^1_{1-1}}{\rho^0_{11} + \rho^0_{1-1}}$$

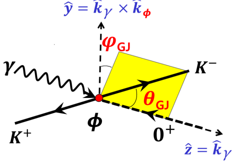

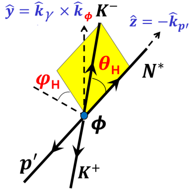

For the helicity-conserving exchanges,

$$\rho^1_{1-1} = -\mathrm{Im}\rho^2_{1-1} = \begin{bmatrix} +0.5(N) \\ -0.5(U) \end{bmatrix}$$

ϕ Photoproduction near Threshold

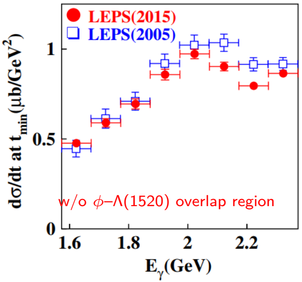

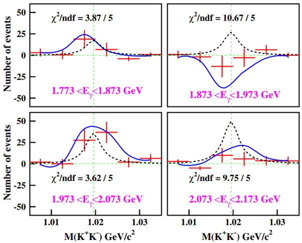

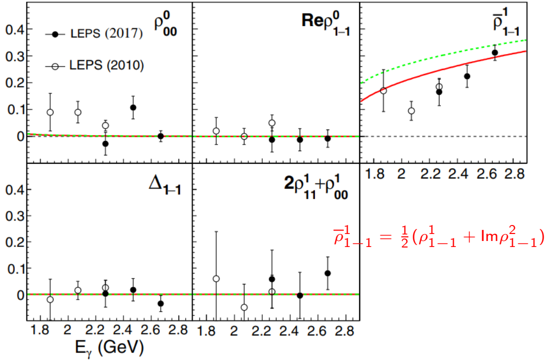

- $\bar{\rho}^1_{1-1}$ deviates largely from the model prediction in $1.97 < E_\gamma < 2.17$ GeV, which reflects the contributions of N^* resonances. [a]
- The $\sqrt{s} = 2.1$ GeV bump structure was reconfirmed without the ϕ–Λ(1520) interference region. [b]

[a] K. Mizutani *et al.*, PRC 96, 062201(*R*)(2017).

[b] S.Y. Ryu *et al.* (LEPS Collab), PRL 116, 232001(2016).

GeV Photon Beam at LEPS2/SPring-8

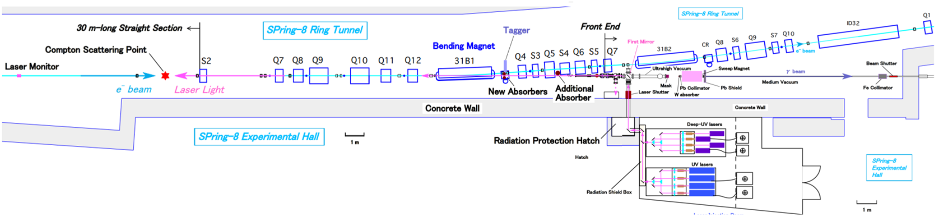

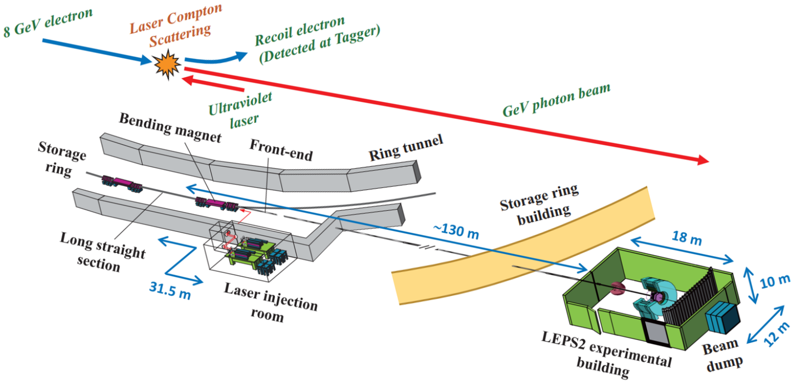

Backward Compton Scattered Photons

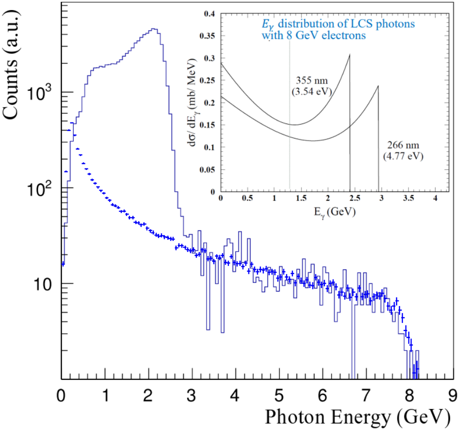

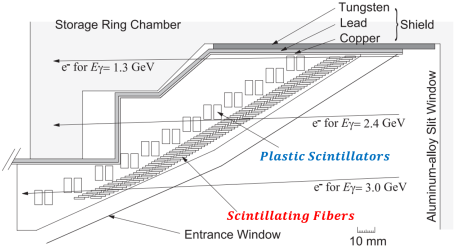

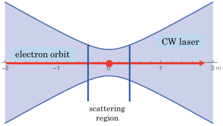

CW laser

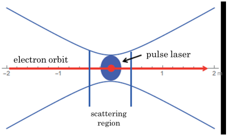

Synchronized pulse laser

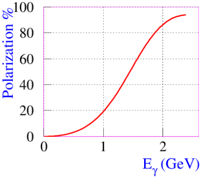

- The tagged photon energy resolution is 12.3 MeV and the maximum intensity is 2.3×10^6/s in the energy from 1.3 to 2.4 GeV. [a]

[a] N. Muramatsu *et al.*, NIMA 1033, 166677(2022).

LEPS2 BGOegg Detector

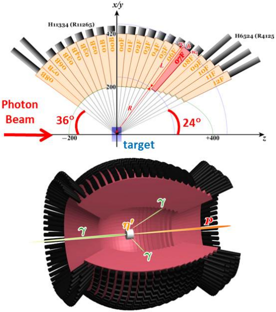

2γ invariant mass spectrum

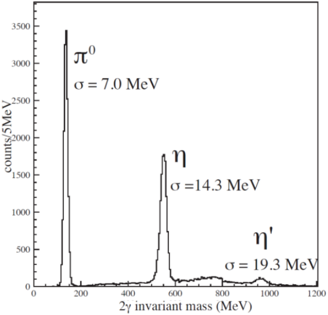

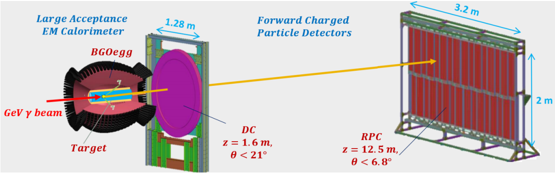

- BGOegg consisting of 1320 BGO crystals (20 X_0) views a target in $\theta = 24° - 144°$ with the world's best energy resolution (1.3% at 1 GeV).[a]

[a] T. Ishikawa *et al.*, NIMA 837, 109(2016).

ω Photoproduction with BGOegg Detector

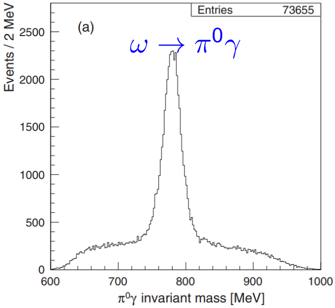

$\gamma p \to \omega p$

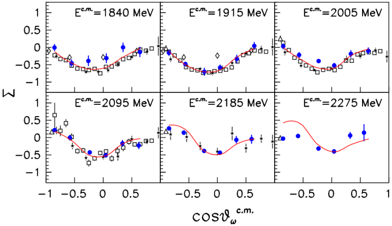

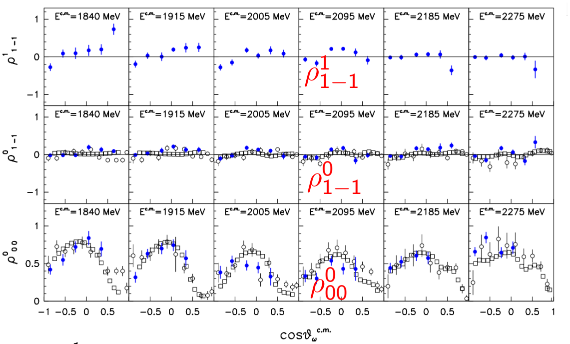

- ρ^1_{1-1} values decrease at forward angles as a function of total energy.
- The ρ^0_{00} shows large values at intermediate angles, while an increase toward higher energies is seen at backward angles.
- The observed behaviors of the helicity-flip amplitudes surely reflects the contributions of N^* resonances. [a]

[a] N. Muramatsu *et al.* (LEPS2 Collab), PRC 102, 025201(2020)

η Photoproduction with BGOegg Detector

$\frac{d\sigma}{d\Omega}$

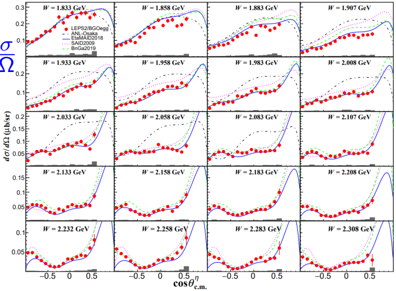

Σ

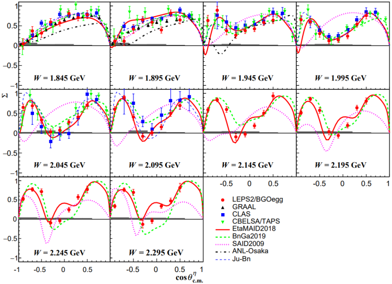

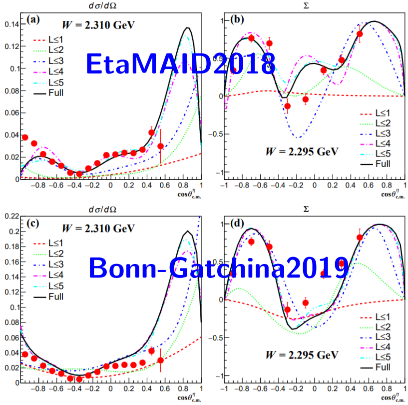

- A bump structure at $W = 2.0$–2.3 GeV is confirmed at extremely backward η polar angles.
- This bump structure is likely associated with high-spin resonances that couple with $s\bar{s}$ quarks. [a]

[a] T. Hashimoto *et al.* (LEPS2/BGOegg Collab), PRC 106, 035201 (2022).

LEPS2 Solenoid Detector

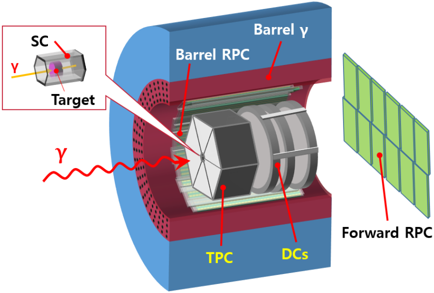

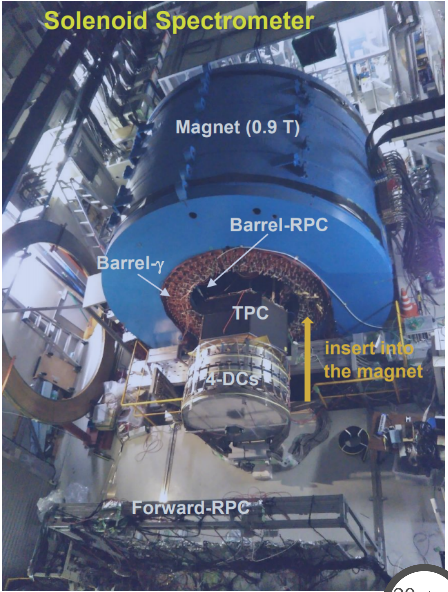

- The LEPS2 solenoid detector comprises TPC, SC, DCs, forward and barrel RPCs, Barrel Pb/Scint calorimeter (14.3 X_0), and neutron counters as well as a photon tagger placed approximately 150 m upstream from the detector.

LEPS2 DAQ System

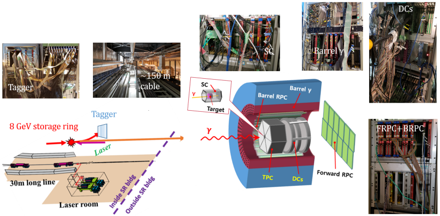

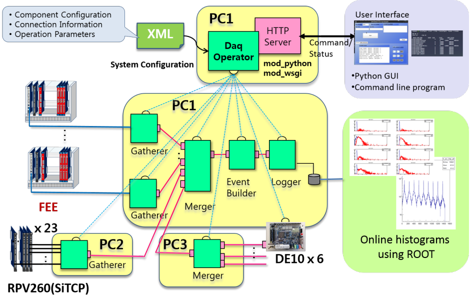

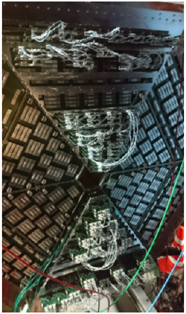

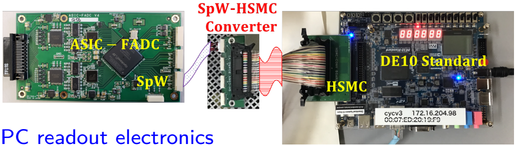

TPC readout electronics

- We have developed a new, network-distributed data acquisition system based on DAQ-middleware framework.[a]

[a] S. Y. Ryu for LEPS2 Collab., AIP Conf. Proc. 2249, 030024 (2020).

Time Projection Chamber

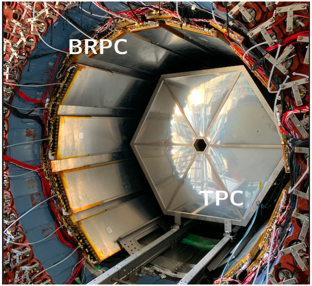

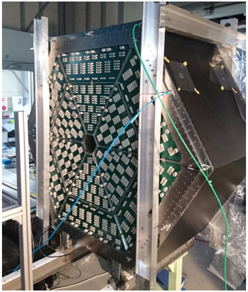

- Hexagonal prism-shaped drift volume : 112 cm (corner-to-corner) $\times$ 71 cm (length).
- 24 straight pad layers grouped into 6 sections forming a hexagonal web-like structure.
- $10,830$ pads with single pad size of 4.6×10 mm^2.

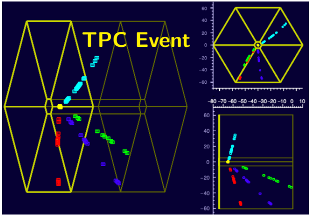

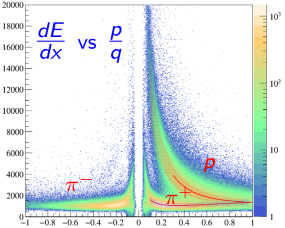

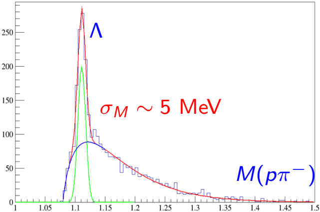

- Λ decays are successfully reconstructed with p and π^- tracks in the first dataset.[a]

[a] R. Kobayakawa for LEPS2 Collab. JPS fall meeting, 2021.

Strange Partner P_s of P_c Pentaquark States

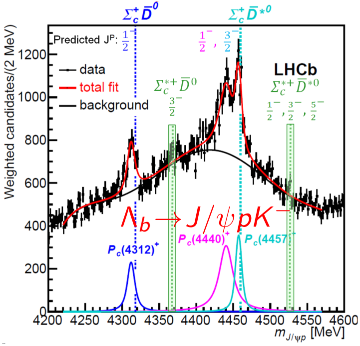

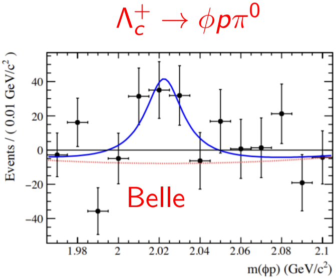

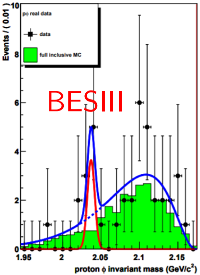

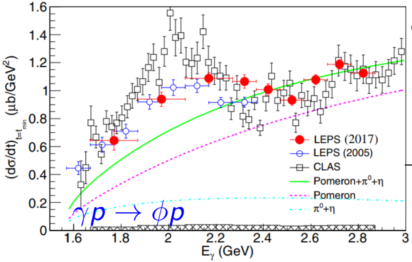

- A strange partner $P_s(uuds\bar{s})$ was searched for in the Cabibbo-suppressed $\Lambda_c^+ \to \phi p \pi^0$ decay at Belle[a] and BESIII.[b] $(\mathcal{B}(\Lambda_c^+ \to P_s \pi^0) \cdot \mathcal{B}(P_s \to \phi p) < 8.3 \times 10^{-5}$ at 90% CL)

[a] B. Pal *et al.* (Belle Collab), PRD 96, 051102 (2017).

[b] G. Mezzadri, Ph.D thesis, Ferrada U (2018).

Strange Partner of P_c Pentaquark States

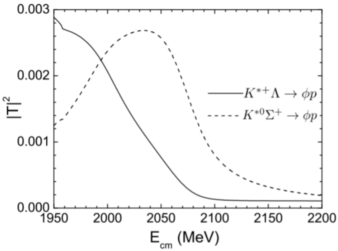

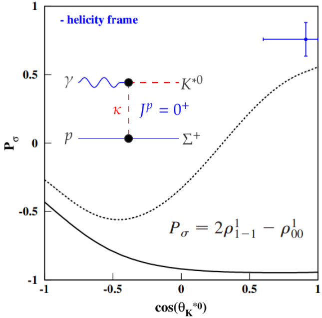

- The bump structure observed in ϕ photoproduction could be regarded as a ΣK^* molecular state ($J = 3/2^-$). Triangular singularity could also explain the bump structure with $\Sigma K^* \to \phi p$.[a]

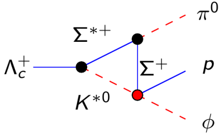

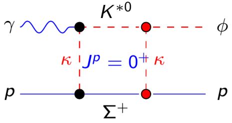

- The measured parity spin asymmetry shows that natural-parity exchange is dominant in $\gamma p \to K^{*0}\Sigma^+$ reaction.[b]
- The nature of the bump structure should be further investigated using circularly polarized photon beam and a polarized (HD) target.

[a] J-J. Xie and F-K Guo, PLB 774, 108 (2017); J. He, PRD 95, 074031(2017).
[b] S.H. Hwang *et al.* (LEPS Collab.), PRL 108, 092001(2012).

Θ^+ Search at LEPS2

- We search for the $\Theta^+(S=+1,\, uudd\bar{s})$ via $\gamma d \to K^- K^0 pp$ reaction, followed by $\Theta^+ \to K^0 p;\ K^0(K_S) \to \pi^+\pi^-$.
- All final state particles can be reconstructed using the large-acceptance LEPS2 detector, which facilitate a wider angular coverage for K^- detection.

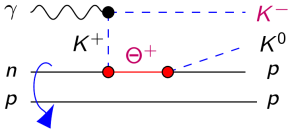

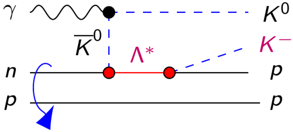

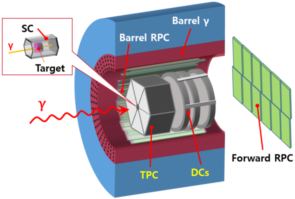

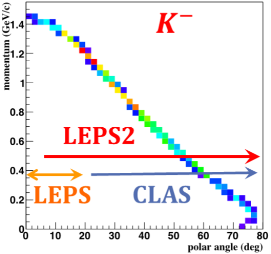

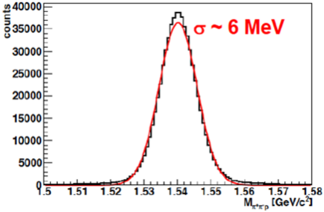

Photoproduction of $\Lambda(1405)$ with K^{*+}

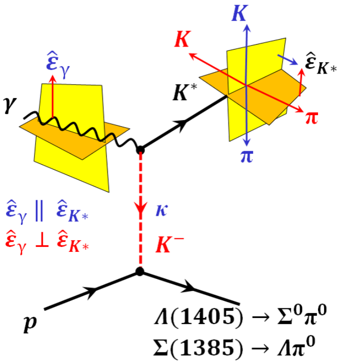

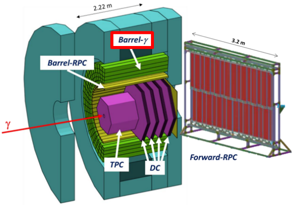

- $K^{*+}(\to \pi^+ K^0_S)$ decay plane $\perp$($\parallel$) the photon beam polarization ($\hat{\varepsilon}$) for unnatural-parity exchange (natural-parity exchange)
- Unnatural-parity K^- exchange selects $\Lambda(1405)$ strongly coupled to a K^-p pole .[a]
- $I = 0$ channel $\Lambda(1405) \to \Sigma^0\pi^0$ can be reconstructed using Barrel-γ detector.

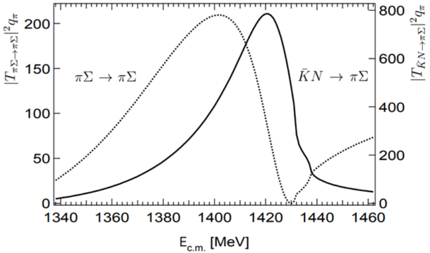

[a] Jido *et al.*, NPA 725, 181 (2003); T. Hyodo *et al.*, PLB 593, 75 (2004).

Search for K^-pp nuclei at LEPS2

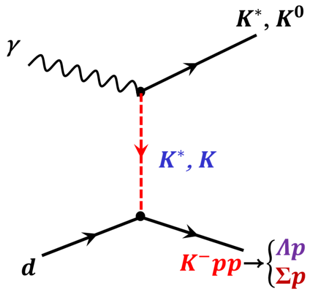

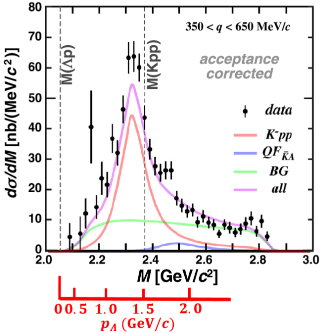

- J-PARC E15 reported a peak in Λp mass of ^{3}He$(K^-, \Lambda p)n$ well below K^-pp mass threshold. [a]
- K^-pp search in $\gamma d \to K^+\pi^-X$, $K^0_S X$, and $K^{*0}X$ reactions at LEPS2. facilitating complete kinematics with a detection of K/K^* and decay products from K^-pp.
- The existence of K^-pp nuclei can also be reconfirmed with Λp scattering in the range of 0.5–2.0 GeV$/c$.

$$\gamma p \to K^+\Lambda \; ; \quad \Lambda p \to (K^-pp) \to \Lambda p$$

[a] J-PARC E15 Collab., Phys. Lett. B 789, 620 (2019).

Summary

- A LEPS2 facility with BGOegg and solenoid detectors has started its full operation for studying hadron spectroscopy from photoproduction using high-intensity Compton backscattered photons at SPring-8.
- Highly polarized photons are very powerful to unveil the nature of hadrons from photoproduction; N^*, Δ, Λ^*, Σ^*, Θ^+, P_s, $K^- pp$ and so on.
- The LEPS2 solenoid detector has completed its first phase of physics runs. Analysis effort of the first dataset is now underway. Please stay tuned.